TIME-FREQUENCY ANALYSIS OF INTERMITTENT TWO-PHASE FLOWS IN HORIZONTAL PIPING

Fabiana Lopes Klein
NETeF- EESC-Universidade de São Paulo
Av. Trabalhador São Carlense, 400
CEP: 13566-590 São Carlos,SP. Brazil
Fabiana_lopes@hotmail.com

Paulo Seleghim Junior
NETeF- EESC-Universidade de São Paulo
Av. Trabalhador São Carlense, 400
CEP: 13566-590 São Carlos,SP. Brazil
seleghim@sc.usp.br

Eric Hervieu
DTP-DRN-Commissariat à l'Energie Atomique
38054 Grenoble cedex 9. France
hervieu@dtp.cea.fr

Abstract. One of the main features associated to multiphase flows is the existence of characteristic dynamic structures according to which the different phases of a mixture of immiscible fluids can flow. The manifestation of one of these structures, known a flow pattern or regime, is determined by the flow rates as well as by physical and geometrical properties of the fluids and piping. The development of flow pattern characterization and diagnostic methods, and the associated transitions in between, is of crucial importance for an efficient engineering of such phenomena. Time-frequency analysis based on the Gabor transform is used in this work to characterize horizontal air-water intermittent flow regimes. More specifically, our main objective is to reveal the existence of sub-regimes inside the intermittent regimes region with the help of the corresponding time-frequency covariance based on the Gabor transform, which is capable of detecting transitions by assessing the unstationarity associated with the corresponding transitions. Experimental testes were conducted at the TALC facility at CEA-Grenoble and an extensive database was obtained, covering several types of intermittent flow. A conductivity probe, consisting in two ring electrodes flush mounted to the pipe, delivered signals from which the time-frequency covariance were calculated from the corresponding Gabor transform.

Keywords: multiphase flow; flow regimes; time-frequency; intermittent

1. Introduction

One of the main features associated to multiphase flows is the existence of characteristic dynamic structures according to which the different phases of a mixture of immiscible fluids can flow. The manifestation of one of these structures, known as flow pattern or regime, is determined by the flow rates as well as by physical and geometrical properties of the fluids and piping. From a practical point of view, the main implication of these regimes refers to their strong influence in important operation parameters such as pressure drop, reaction and diffusion rates, etc. During the design stage of a specific application involving multiphase flow, physical models capable of predicting the types of regime and the conditions they will be present are of crucial importance for their correct and efficient engineering. Subsequently, during the operation stage, the flow regimes for which the application has been designed must be monitored to assure their existence or to launch countermeasures if an undesired or possibly dangerous flow regime is detected. Therefore, not only the development of physical models for multiphase flow regimes, which were initially based on visual observation, but also the corresponding detection methodologies depend on the development of new objective flow regime characterization techniques.

The development of objective detection criteria for multiphase flow regimes has been the central research subject among many researchers during the recent past. Probably one of the first research works on this subject is the one by Hubbard and Dukler (1966) in which different flow regimes were characterized through their spectral signatures of temporal pressure signals. Also can be evoked the works by Weisman et al. (1979), Vince and Lahey (1982), Matsui (1984), Tutu (1984), Mishima and Ishii (1984), Sekoguchi et al. (1987) and many others. An important review work providing an extensive compilation of the research work during the 70's and 80's is the article by Drahos and Cermak (1989). The tendency in the 90's was to investigate the use of fractal methods and less restrictive signal analysis techniques, such as adaptative filtering and wavelets. Regarding specifically the characterization of the flow patterns from its fractal and/or chaotic aspects, Saether et al. (1990), França et al. (1991) and Lewin (1992) proposed interesting

flow pattern characterization methods based on the determination of fractal dimensions. Also Giona et al. (1994) and Soldati et al. (1996) proposed the use of diffusional analysis as an adequate method for the characterization of flow regimes and their transitions in horizontal gas-liquid flows. In what concerns more specifically two-phase fluid mechanics, Hervieu and Leducq (1991) demonstrated the potential of the wavelet transform to characterize vertical flow regimes. Later, Seleghim and Hervieu (1994) proposed an objective indicator for the bubbly to slug transition in vertical flow, based on the quantification of the loss of stationarity through the standard deviation of Ville's instantaneous frequency. Finally, Hervieu and Seleghim (1998) optimized the proposed criterion in the sense of making it universal, i.e. independent of the transition and of the analyzed signal, and proposed the use of the time-frequency covariance calculated from the signal's Gabor transform as a new flow regime transition indicator.

The main objective of this work is to investigate the existence of sub-regimes within the intermittent flow region of horizontal gas-liquid flows. This will be done with the help of time-frequency covariances calculated from the Gabor transform of void signals obtained from an electrical impedance probe. The text is organized as follows: a) description of the basic concepts associated with time-frequency analysis, Gabor transform and the information that can be extracted from time-frequency covariance, b) description of the experimental facilities and the instrumentation used in this work, c) details concerning the experimental tests, their analysis and results, and d) conclusions and perspectives for future research work.

2. Basic Concepts of Time-Frequency Analysis

The analysis of the frequency content of a signal, based exclusively on its Fourier Transform, may fail to completely describe the process or physical phenomena because all temporal information is masked due to the integration in time. In other words, if a signal is composed of different frequencies existing in different periods of time, that is its spectral content evolves in time, it is necessary to analyze it simultaneously in time and frequency. A power density distribution calculated from the signal and capable of identifying its frequencies and the corresponding periods in which they existed is called a joint time-frequency representation of the signal.

There are several strategies to obtain such alternative representations. One interesting approach consists in using a sliding window function to stress temporal features in particular regions of time. More precisely if $s(\tau)$ denotes the original signal and $h_t(\tau)$ denotes the window function centered in $\tau = t$ with implicit duration given by T, it is possible to define a modified signal $s_t(\tau)$

$$s_t(\tau) = s(\tau) \cdot h_t(\tau) \tag{1}$$

The modified signal depends on three times: the support τ, the instant of analysis t and the implicit length or horizon of analysis T. Since the temporal aspects of the original signal are emphasized around t in the modified signal, the Fourier Transform of this last will reflect the spectral composition around the same instant of analysis, that is

$$S_t(\omega) = \frac{1}{\sqrt{2\pi}} \int_{-\infty}^{+\infty} s_t(\tau) \exp(-i\omega\tau) d\tau \tag{2}$$

Or, by replacing definition (1), it is possible to obtain

$$S_t(\omega) = \frac{1}{\sqrt{2\pi}} \int_{-\infty}^{+\infty} s(\tau) h(\tau) \exp(-i\omega\tau) d\tau \tag{3}$$

The corresponding joint time-frequency spectral density $P(t,\omega)$ can be defined according with the following formula

$$P(t,\omega) = \| S_t(\omega) \| = \left| \frac{1}{\sqrt{2\pi}} \int_{-\infty}^{+\infty} s(\tau) h(\tau) \exp(-i\omega\tau) d\tau \right|^2 \tag{4}$$

To illustrate the ability of $P(t,\omega)$ in extracting the frequency content at given instant of analysis, consider the linear chirp given by

$$s(\tau) = \cos[\alpha(\tau)\tau] \quad \text{with} \quad \alpha(\tau) = \omega_0 |(1+\tau)| \tag{5}$$

The characteristics of this signal are so that it is clear that its spectral content must be centered at the instantaneous frequency given by $\alpha(t)$. Also, by adopting a rectangular window with duration containing at least a few oscillations of the linear chirp, the corresponding joint time-frequency spectral density $P(t,\omega)$ can be calculated through Eq. (4) and plotted in function of the instant and frequency of analysis.

This type of joint time-frequency spectral density $P(t,\omega)$ is usually called Short Time Fourier Transform (STFT) or simply a spectrogram. An important STFT is the Gabor Transform, obtained by adopting a Gaussian function as the analyzing window, which has very interesting mathematical properties such as the ease in optimizing simultaneously the temporal and frequency resolutions. Other types of joint time-frequency distributions can be obtained through different approaches. For instance, the Wigner-Ville distribution is constructed from the Fourier transform of the Ambiguity function and the wavelet transform is obtained by affine transforming an analyzing function with a well defined central frequency and time (a wavelet).

Time-frequency analysis constitutes an important framework for assessing the unstationarity of a signal or process. More precisely, in the context of deterministic processes, stationarity is generally assumed to be a spectral state in which the frequency composition is constant with respect to time (Flindrin, 1993; Hervieu and Seleghim, 1998).

This implies that $P(t,\omega)$ is strictly independent of time or, admitting a slow modulation $f(t)$ of the spectral amplitudes envelope $G(\omega)$, that $P(t,\omega)$ can be written as

$$P(t,\omega) = f(t)G(\omega) \tag{6}$$

How slow means a slow modulation can be established with the help of Bedrosian's theorem, that is, that the supports of the Fourier transform of $f(t)$, denoted by $F(\omega)$, and of $G(\omega)$ are approximately disjoint:

$$\sup p[F(\omega)] \cap \sup p[G(\omega)] \cong \varnothing \tag{7}$$

This being, unstationarity can be quantified by measuring how well a specific joint function could be represented by separable functions. In precise terms, if $S \subset L^2(R^2)$ is the subspace of all separable joint functions, unstationarity can be assessed through the distance between $P(t,\omega)$ and its projection into S. However, this is not as easy as it seems because very little is known about S, even if it exists for a given class of joint functions. But plausible arguments can be evoked to construct an adequate metrics satisfying some of the requirements of an unstationarity quantifier. For instance, if stationarity implies that the central frequency and central time calculated from $P(t,\omega)$ are uncorrelated, its normalized time-frequency covariance should indicate how unstationary the original signal or process is. Thus, by defining a proper analysis horizon T, a central frequency $\Delta_\omega(\tau)$, a central time $\Delta_t(\tau)$ and a joint moment $\Delta_{t\omega}(\tau)$ such as

$$\Delta_\omega(\tau) = \frac{1}{E_s} \int_{-\infty}^{+\infty} \int_{-\tau+\frac{T}{2}}^{-\tau+\frac{T}{2}} \omega P(t,\omega)\, dt\, d\omega \tag{8}$$

$$\Delta_t(\tau) = \frac{1}{E_s} \int_{-\infty}^{+\infty} \int_{-\tau+\frac{T}{2}}^{-\tau+\frac{T}{2}} t P(t,\omega)\, dt\, d\omega \tag{9}$$

$$\Delta_{t\omega}(\tau) = \frac{1}{E_s} \int_{-\infty}^{+\infty} \int_{-\tau+\frac{T}{2}}^{-\tau+\frac{T}{2}} t\omega P(t,\omega)\, dt\, d\omega \tag{10}$$

in which E_s represents the energy of $P(t,\omega)$ calculated inside the limits of integration of (8) and (9), it is possible to define the joint time-frequency covariance in analogy with the concept from mathematical probability:

$$\text{cov}(\tau) = \left| \Delta_{t\omega}(\tau) - \Delta_t(\tau)\Delta_\omega(\tau) \right| \tag{11}$$

Expression (11) is a very convenient definition in what regards the deterministic stationarity. For instance, if $P(t,\omega)$ is separable and satisfies (6), the calculus of the corresponding time-frequency covariance leads to

$$\text{cov}(\tau) \;=\; \frac{1}{E_s}\left| \int_{-\infty}^{+\infty} \int_{-\tau+\frac{T}{2}}^{-\tau+\frac{T}{2}} t\,\omega\,P(t,\omega)\,dt\,d\omega - \int_{-\infty}^{+\infty} \int_{-\tau+\frac{T}{2}}^{-\tau+\frac{T}{2}} t\,P(t,\omega)\,dt\,d\omega \int_{-\infty}^{+\infty} \int_{-\tau+\frac{T}{2}}^{-\tau+\frac{T}{2}} \omega\,P(t,\omega)\,dt\,d\omega \right| \tag{12}$$

By introducing (6) and after integrating separately in t and ω, expression (12) simplifies to

$$\text{cov}(\tau) \;=\; \frac{1}{E_s}\left| \int_{-\infty}^{+\infty} \omega\,G(\omega)\,d\omega \int_{-\tau+\frac{T}{2}}^{-\tau+\frac{T}{2}} t\,f(t)\,dt - \int_{-\infty}^{+\infty} \omega\,G(\omega)\,d\omega \int_{-\tau+\frac{T}{2}}^{-\tau+\frac{T}{2}} t\,f(t)\,dt \right| \;=\; 0 \tag{13}$$

That is, if the original signal is stationary the corresponding $P(t,\omega)$ is separable and the associated time-frequency covariance is zero. It is also possible to demonstrate that if there is a maximum coupling between the central time and frequency, what implies that the spectral content of the original signal is varying and it is, thus, unstationary, the associated joint time-frequency covariance attains a maximum. This can be illustrated by the following analytical example:

$$P(t,\omega) \;=\; \exp\left\{ -\frac{1}{a}\left[(t-t_0)\cos\theta + (\omega-\omega_0)\sin\theta\right]^2 - \frac{1}{b}\left[(t_0-t)\sin\theta + (\omega_0-\omega)\cos\theta\right]^2 \right\} \tag{14}$$

In the Eq. (14) the argument θ determines the coupling between the corresponding Δ_t and Δ_ω (if $\theta=0$ or $\theta=90^0$ Δ_t and Δ_ω are uncorrelated and if $\theta=\pm 45^0$ the correlation between Δ_t and Δ_ω is maximum). Adopting an infinite horizon of analysis $(T\to\infty)$ and introducing Eq. (14) into the definition Eq. (11), through Eqs. (08), (09) and (10), results in

$$\text{cov}(\tau) \;=\; a\,b\,\frac{\sin(2\theta)}{4} \tag{15}$$

which obviously experiences a maximum for $\theta=\pm 45^0$ and a minimum for $\theta=0$ or $\theta=90^0$.

3. The experimental circuit

The search for sub-regimes within the intermittent flow region was carried out experimentally through extensive experimental tests performed at the Commissariat a l'Energie Atomique, in Grenoble, France. Void fraction signals were obtained from a conductivity probe installed on a horizontal two-phase flow loop basically composed of an air circuit, a water circuit, a mixer, a test section and a separator, as illustrated in the next Figure 1.
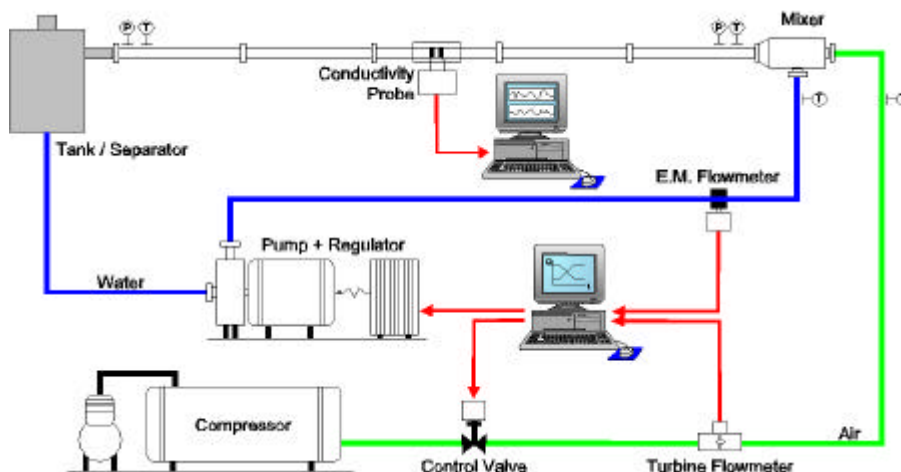
Figure1: Experimental test loop at the CEA – Grenoble, France

The test section, made in Plexiglas to allow flow visualization, is 30m long and has an internal diameter of 60mm. Special supports were designed in order to satisfy three basic requirements: dynamic neutrality (hydrodynamic forces do not generate mechanical vibrations), thermal stress compensation and possibility to incline the test section. A laser beam and a set of targets placed along the test section control its alignment and horizontality. The global misalignment does not exceed 3mm over the total length. The instrumentation of the loop includes temperature and pressure transducers and electromagnetic and turbine flow meters to measure respectively water and air flow rates. Two independent PID based regulation loops control each of the flow rates, and allow to impose their temporal variations. It is important to stress that a careful choice of the PID parameters is fundamental for the performance of the loop both in transient as well as in steady-state operation. This is related to the fact that the dynamic behavior of the two-phase loop depends on the flow pattern which can change abruptly and entirely during a transient test. A detailed description of the loop is provided by Seleghim, 1996.

3.1. The conductivity probe

In order to identify a flow regime transition by quantifying the deviation from deterministic stationarity, it is necessary to measure variations in the spectral content of a signal, which must carry information concerning the flow patterns and the associated dynamic stability. Local interfacial area or void fraction are possible signals and can be easily determined by using a resistive impedance measurement technique. Since the proposed diagnostic method lies more on spectral features than on absolute values of the signal, a special electrode configuration was adopted, composed of an exciting ring and a measurement ring mounted flush in the tube. This produces conductivity signals whose mean value is related to the void fraction by a factor depending only on the flow regime (Andreussi et al., 1988, Seleghim and Hervieu1 1998). The configuration of the probe as well as the conditioning electronics is depicted in the following Figure 2.
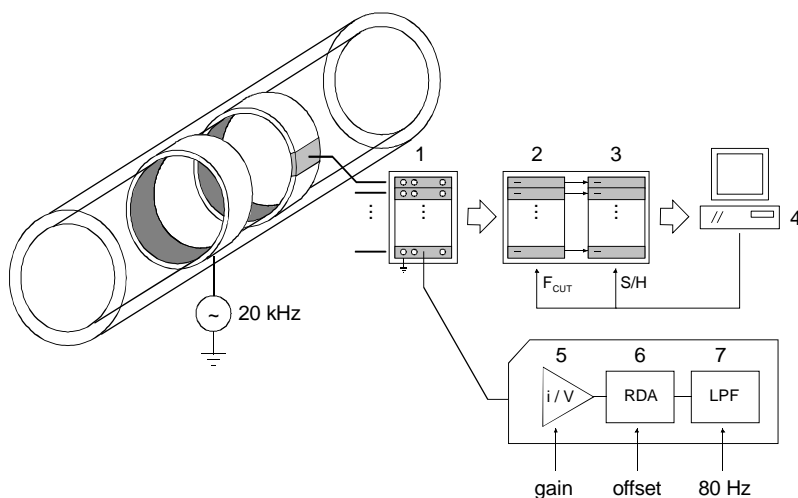

Figure 2: Conductivity probe, conditioning electronics and data acquisition system

The measurement system has 16 independent input channels and is basically composed of the current to voltage transducer modules, a signal conditioning chassis (National Instruments SCXI-1001) equipped with anti-aliasing filters (SCXI-1141) in series with sample and hold circuits (SCXI-1140) and, an acquisition board (National Instruments AT-MIO-16E-5) installed on a microcomputer. This is depicted in figure 4, which also reveals some details: current / voltage transducer (1), anti-aliasing filters (2), sample and hold circuits (3), microcomputer with acquisition board (4), current to voltage converter with gain control (5), rectifier with offset control (6) and forth-order low-pass Butterworth filter with $f_{cut} = 80Hz$ (7).

This measurement system is capable of producing qualitative images of the flow by simply plotting the output current of each electrode in function of time (horizontal scale) and its angular position (vertical scale). These images are very rich not only on large two-phase structures but also on fine details of the geometry of the phases. This is illustrated in the next figure for annular and intermittent flow, in which the output current is coded in colour levels, white corresponding to zero (void fraction is equal to one) and black corresponding to the maximum value (void fraction is equal to zero). In figure 3(a), annular flow, it is possible to observe the parietal liquid film and that its thickness increases at the bottom of the tube. It is also possible to observe the regular passage of toroidal waves. In the intermittent flow illustrated in figure 3(b) it is possible to notice the ripple waves at the bottom of the air plugs, some of which have biconvex tails. The regular modulation of the intermittency frequency can also be inferred from this image.
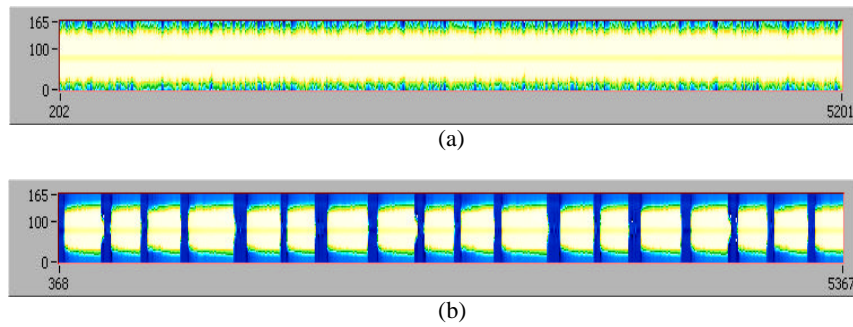

(a)

(b)

Figure 3: Qualitative images delivered by the conductivity probe (a: annular flow and b: intermittent flow)

4. Experimental Tests and Results

An extensive series of long duration steady state tests was conducted aiming to reveal the existence of a transition within the intermittent flow regime region at the experimental loop described above. The base signals correspond to the sum of the output current of each of the sensing electrodes of the direct imaging probe (Figure 2), which corresponds to the global inter-electrode conductivity and is closely related to the instantaneous volumetric void fraction. The signals were also anti-aliasing filtered and sampled at 100Hz. Denoting Q_l and Q_g respectively the liquid and the gas volumetric flow rates (at normal conditions), the explored flow ranges correspond to Q_l minima = 0.5m³/h, Q_l maxima = 50m³/h, Q_g minima = 6m³/h e Q_g maxima = 250m³/h. These values and the full operation envelop of the experimental loop are shown in the flow chart of the following figure (Taitel & Dukler, 1976). The exact flow rate values of each test are given in the following table.
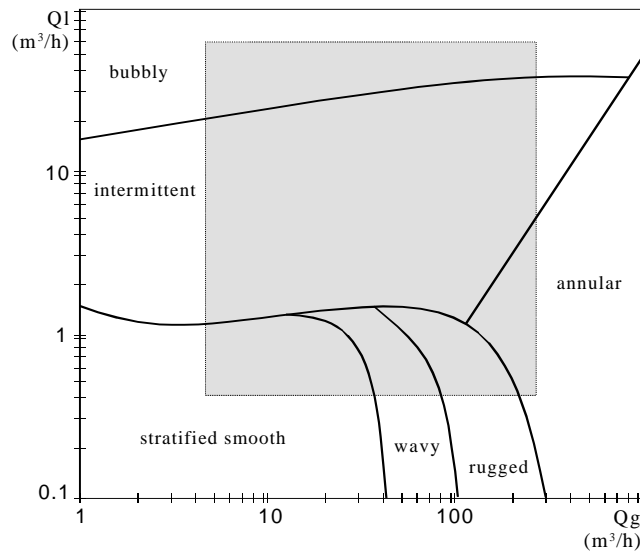

Figure 4: Taitel and Dukler`s (1976) flow chart with indication of the series of long duration steady state tests conducted in this work. The gray region corresponds to full operation envelop of the experimental loop of Figure 1

Table 1: Gas and liquid volumetric flow rate (normal conditions) and test labels.

Experimental Test	Q_g (m^3/h)	Q_l (m^3/h)
Test 1	14.5	5.02
Test 2	16.2	6.00
Test 3	16.2	7.04
Test 4	16.7	6.97
Test 5	18.4	5.95
Test 6	20.0	4.94
Test 7	23.6	3.99
Test 8	24.8	5.04

The intermittent flow structures corresponding to tests 1 through 8 can be visualized by plotting the normalized output current of each sensing electrode in function of time (horizontal scale) and its angular position (vertical scale). This is done in Figure 5, in which gray levels indicate the local void fraction (white corresponds to air and black corresponds to water). As it can be seen, the intermittent flow regime is characterized by the alternate passage of large gas bubbles or plugs separated by liquid lumps, which can be more or less aerated depending on the group velocity of the structures. Under these conditions, the conductivity signals will oscillate between two characteristic levels with an average periodicity reflecting the intermittency frequency of the flow.

(a) Test 1

(b) Test 2

(c) Test 3

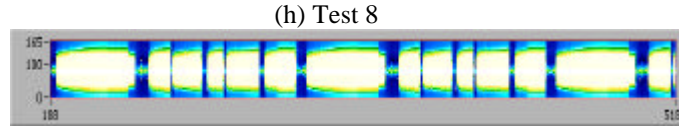(d) Test 4

(e) Test 5
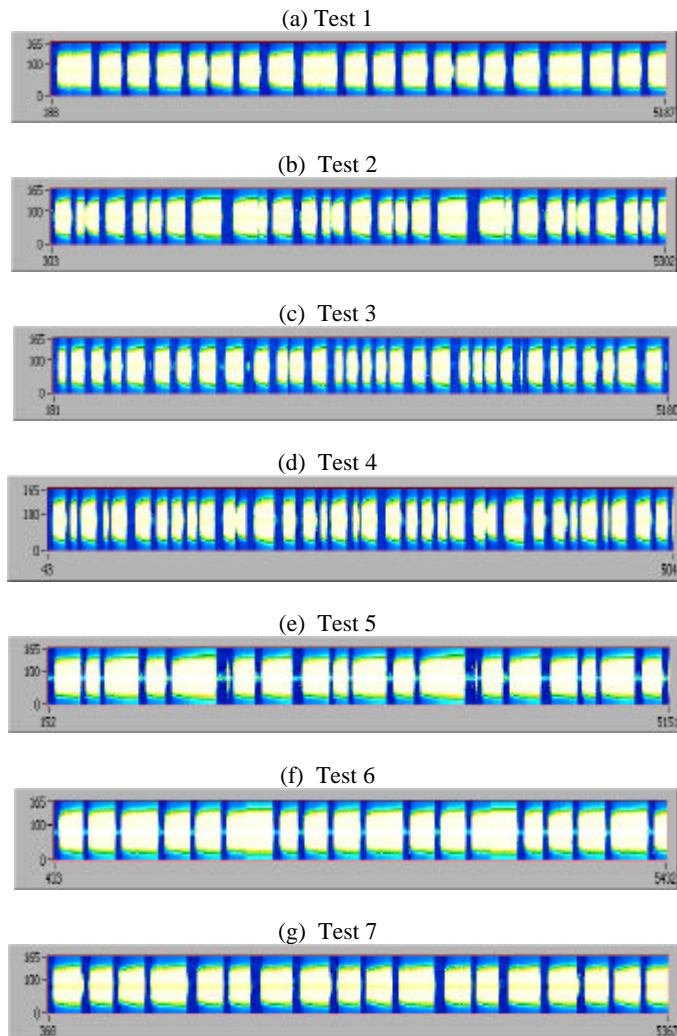
(f) Test 6

(g) Test 7

Figure 5: Direct images of the flow regimes of testes 1 through 8. Colour levels map the local void fraction (white represents air and black represents water)

The images in Figures 5(a) and 5(g) (tests 1 and 7) are highly stationary intermittent flow, with non-aerated water slugs, for which the intermittency frequency is particularly stable. Opposing to this, the image in Figure 5(b) (test 2) shows a situation in which some of air plugs are closer to each other due to the effect of their wakes and some of the air plugs are more spread out (the accordion effect). As a consequence of this, the stability of the flow decreases and the intermittency frequency oscillates, indicating a possible regime transition. This unstable behavior is also observed in Figures 5(c) and 5(d) (tests 3 and 4). In the subsequent tests the distance between the air plugs is roughly constant, except for the Figure 5(h) (test 8) for which a sequence of small plugs is followed by large elongated bubbles with biconvex tails, indicating possibly a new regime transition.

The oscillation of the intermittency frequency can be more accurately visualized with the help of a joint time-frequency distribution, such as the Gabor transform described before, and the corresponding joint time-frequency covariance. As already mentioned the time-frequency covariance reflects the unstationarity level of the signal and constitutes an objective flow regime transition indicator (Hervieu and Seleghim, 1998). Thus, transition flows are characterized by high covariance values compared with the corresponding ones obtained from well established flows. The following figure shows the time-frequency covariance calculated from the Gabor transform of each of the signals corresponding to tests 1 through 8, as defined in Table 1.
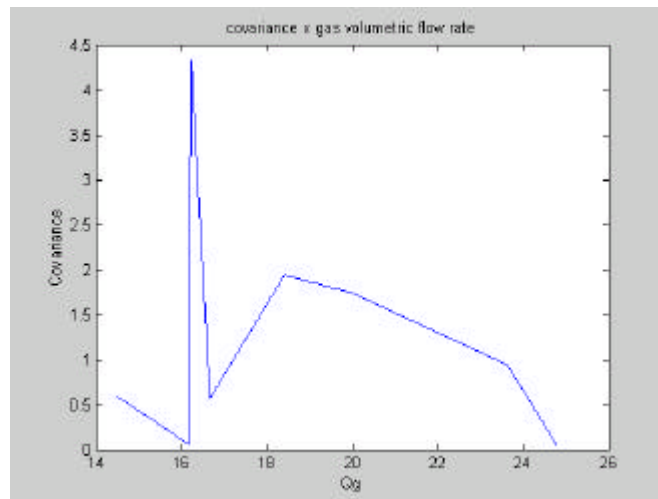

Figure 6: Time-frequency covariance calculated from the Gabor transform of each of the signals corresponding to tests 1 through 8

It can be observed that the test 3 (Figure 5(c)) is the most unstationary and possibly corresponds to a transition between two types of intermittent flow. The high unstationarity level of this particular test reflects the strong oscillation of its intermittency frequency, what is closely related to the accordion effect. The following figure shows the Gabor transform of global conductivity signal of test 3, where the trajectory of the central frequency (the gray ridges) falls between 0.4 and 0.9Hz, which is approximately the modulation law associated with the intermittency frequency.
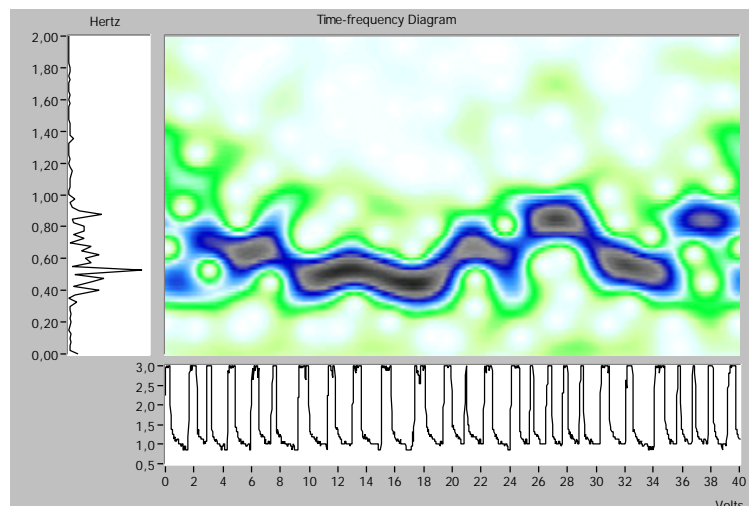
Figure 7: Gabor transform of the conductivity signal of test 3 (Figure 5(c)) – central diagram is the amplitude of the Gabor transform coded in gray levels, the lower plot is the conductivity signal plotted in function of time, and the plot on the left is its Fourier transform plotted in function of the analyzing frequency

5. Conclusions and Perspectives

In this work we investigated the existence of sub-regimes within the intermittent flow regime operation region of a horizontal air-water flow. This was done with the help of the joint time-frequency covariance, which assesses the level of unstationarity of a signal and constitutes an objective transition indicator (Hervieu and Seleghim, 1998). Experimental tests were conducted at the facilities of the Commissariat à l'Energie Atomique, in Grenoble, France, at its two-phase flow horizontal loop. The test section has an internal diameter of 60mm and is 30m long. The instrumentation includes a multielectrode direct imaging probe, which global conductivity signals are used to characterize the flow regime. The time-frequency covariance of theses signals indicate that an increase of the unstationarity level is associated with the so-called accordion effect, i.e. the successive passage of tighter and looser trains of air plugs. The analysis of the corresponding Gabor transform shows that this effect is characterized by a strong modulation of the intermittency frequency and possibly indicates that the flow regime is transitioning between two different types of intermittent flow. Future work should focus on a more extensive investigation, with experimental tests covering a wider range of the intermittent flow regime operation region of the experimental loop.

6. Acknowledgements

7. References

Andreussi P., Di Donfrancesco A. and Messia M., 1988, "An impedance method for the measurement of liquid hold-up in two-phase flow", International Journal on Multiphase Flow, Vol. 14, No. 6, pp.777-785.

Drahos J. and Cermak, J., 1989, "Diagnostics of Gas-Liquid Flow Patterns in Chemical Engineering Systems", Chemical Engineering Processes, Vol. 26, pp.147-164.

Flindrin, P. (1993). Temps-fréquence. Hermès, Paris.

França, F., Acikgoz, M., Lahey, R. T. Jr. and Clausse, A., 1991, "An Application of Fractal Techniques to Flow Regime Identification", Ed. A. P. Burns, Mult-Phase Production. London, Elsevier Applied Science, pp.281-293.

Giona, M., Paglianti, A. and Soldati, A., 1994, "Diffusional Analysis of Intermittent Flow Transitions", Fractals, Vol. 2, pp. 256-258.

Hervieu, E. and Leducq, D., 1991, "The Wavelet Transform as a Diagnostic Tool in Two-Phase Flows: Characterization of Multiphase Flows From Wall Measurements", European Two-Fhase Flow Group Meeting, Rome.

Hervieu, E. and Seleghim, P. Jr., 1998, "An Objective Indicator for Two-Phase Flow Pattern Transition", Third International Conference on Multiphase Flow, ICMF'98, v.CD-ROM, pp.1-7.

Hubbard, M. G. and Dukler, A. E., 1966, "The Characterization of Flow Regimes for Horizontal Two-Phase Flow", Proc. Heat Transfer and Fluid Mech, Eds. M. A. Saad and J. A. Moller, Stanford University Press.

Lewin D.R., Faigon M., Fuchs A. and Semiat R., 1992, "Modeling and control of two-phase systems", Computational Chemical Engineering, Vol.16, No.6, pp.5149-5146

Matsui G., 1984, "Identification of Flow Regimes in Vertical Gas-Liquid Two-Phase Flow Using Differential Pressure Fluctuations", International Journal Multiphase Flow, Vol. 10, No. 6, pp.711-720.

Mishima, K. and Ishii, M., 1984, "Flow Regime Transition Criteria for Upward Two-Phase Flow in Vertical Tubes", International Journal Heat Mass Transfer, Vol. 27, No. 5, pp.723-737.

Saether G., Bendiksen K., Muller J. and Froland E., 1990, "The fractal statistics of liquid slug lengths", International Journal on Multiphase Flow, Vol.16, No.6, pp.1117-1126.

Sekoguchi, K., Inoue, K. and Imasaka, T., 1987, "Void Signal Analysis and Gas-Liquid Two-Phase Flow Regime Determination by a Statistical Pattern Recognition Method", JSME International Journal, Vol. 30, No. 266, pp.1266-1273.

Seleghim, P. Jr. and Hervieu, E., 1994, "Caractérisation des Changements de Configuration des Écoulements Diphasiques Gaz-Liquide Par Analyse de La Fréquence Instantanée", C. R. Acad. Sci. Paris, t.319, série II, pp.611-616.

Seleghim, P. Jr. and Hervieu, E., 1998, "Direct imaging of two-phase flows by electrical impedance measurements", Meas. S. Technol., Vol. 9: (9), pp.1492-1500.

Seleghim P. Jr., 1996, "Caractérisation des changements de configuration d'un écoulement diphasique horizontal par l'application de méthodes d'analyse temps-fréquence", Phd Thesis, Institut National Polytechnique de Grenoble – France, 528p. (in french)

Soldati, A., Paglianti, A. and Giona, M., 1996, "Identification of Two-Phase Flow Regimes Via Diffusional Analysis of Experimental Time Series", Experiments in Fluids, Vol. 21, No. 3, pp.151-160.

Taitel, Y. and Dukler, A.E., 1976, "A Model for Predicting Flow Regime Transitions in Horizontal and Near Horizontal Gas-Liquid Flow", AIChE Journal, Vol. 22, No. 1, pp. 47-55.

Tutu N.K., 1984, "Pressure drop fluctuations and bubble-slug transition in a vertical two-phase air-water flow", International Journal on Multiphase Flow, Vol. 10, No.2, pp.211-216.

Vince, M. A. and Lahey, R. T. Jr., 1982, "On the Development of An Objective Flow Regime Indicator", International Journal Multiphase Flow, Vol. 8, No. 2, pp.93-124.

Weisman J., Duncan D., Gibson J. and Crawford T., 1979, "Effects of fluid properties and pipe diameter on two-phase flow patterns in horizontal lines", International Journal on Multiphase Flow, Vol.5, pp.437-462.